Multivariable Control Design for the Water Gas Shift Reactor in a Fuel Processor

Subbarao Varigonda, Jonas Eborn, Scott A. Bortoff
United Technologies Research Center, East Hartford, CT 06108, USA.

***Abstract*— The water gas shift (WGS) reactor is an essential component of the fuel processor in fuel cell power plants. The WGS reactor combines CO and H_2O in the reformate stream to produce H_2 and CO_2 in a mildly exothermic, equilibrium limited reaction. Proper regulation of the steam-to-carbon ratio and the operating temperature is critical to achieving adequate CO conversion during transients. We consider the control problem for the high temperature shift reactor of a catalytic partial oxidation (CPO) based natural gas fuel processor in a PEM fuel cell power plant. The manipulated variable is the water injection rate and the measurements available are the inlet and exit temperatures of the reactor and the reformate flow from the CPO reactor and the objective is to maintain proper water content in the inlet and CO conversion in the reactor. A linear state space model is obtained by linearizing a nonlinear dynamic model of the system around an operating point of interest. A multivariable controller is designed using the LQR method. We compare various control architectures by selectively dropping the terms in the multivariable controller. It is shown that the reactor exit temperature measurement improves the observability of the system but has negligible influence on the control performance. Such multivariable control analysis provides a systematic framework for the evaluation of alternative control architectures and the impact of sensors.**

I. Introduction

The fuel processing system (FPS) is an integral part of a fuel cell power plant in applications where hydrogen storage is not a viable option. The FPS reforms a hydrocarbon fuel such as natural gas into a hydrogen rich gas and cleans the reformate of impurities such as carbon monoxide that can poison the electrode catalyst of the fuel cell. Polymer electrolyte membrane (PEM) fuel cells have low CO tolerance and require CO to be reduced to ppm levels (less than 40 ppm) which is typically accomplished by multiple stages of water gas shift reactors followed by preferential oxidation of CO [1]–[4]. A schematic of the FPS using catalytic partial oxidation (CPO or CPOX) reactor is shown Figure 1. Natural gas fuel is mixed with air and passed to the main reformer, the CPOX reactor. The reformate stream from CPOX containing predominantly H_2, CO, CO_2, H_2O and N_2 is cooled by injecting water and sent to the WGS reactors to remove the bulk of CO and to supplement H_2. The reformate from WGS reactors is cooled and mixed with air for further CO clean up in the preferential oxidation (PROX) reactors before being fed to the PEM fuel cell.

Water injection after the reforming step serves not only to cool the reformate to the required inlet temperature level for the WGS reactor, but also to increase the moisture content (steam-to-carbon ratio) and drive the WGS reaction forward

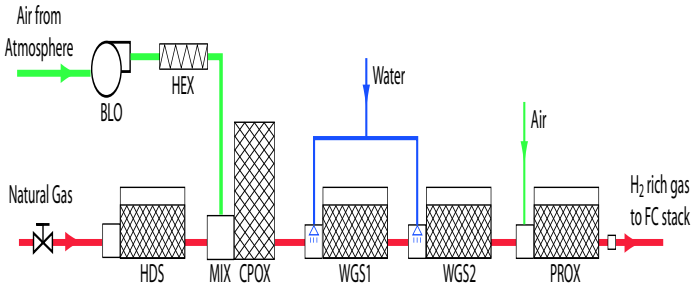

Fig. 1. Schematic of a CPO based fuel processing system in a fuel cell power plant

[3]. The CO conversion in the WGS reactors is limited by the equilibrium of the reaction. Good control of the temperatures is critical to achieving desired CO conversion [4]. Steady state effects of the steam to carbon ratio and the operating temperature on the CO conversion in the shift reactor are reported and design criteria are presented in [3]–[5].

Proper control of CO concentration is required during steady state as well as load transients on the fuel cell system to prevent poisoning of the precious metal catalyst in the fuel cell stack. Our objectives in this paper is to evaluate the closed loop disturbance rejection of the WGS reactor with under multivariable and decentralized control architectures and to assess the impact of the exit temperature measurement on control performance. In particular, we analyze the relative impact of inlet and outlet temperatures and the reformate inlet flow measurements on control performance. The reformate inlet flow is considered as a measured disturbance available as a feedforward signal to the controller but in practice, any upstream measurement with similar information can be used. The manipulated input is the water injection rate.

Although there is a large body of literature on steady state issues in the design and operation of FPS and WGS (see, *e.g.*, [1]–[5]), the work on transient issues and control in the context of fuel cell systems is scarce. A control scheme for the WGS reactor that regulates the inlet gas or water supply and/or inlet temperature based on the measurement of exit CO concentration and possibly the reactor temperature has been disclosed in the patent application [6]. The control for WGS reactor has been studied in [7]. A cascade control architecture with an inner loop controlling the WGS reactor inlet temperature and the outer loop controlling a temperature close to the exit was considered in [7] and the performance of various gain

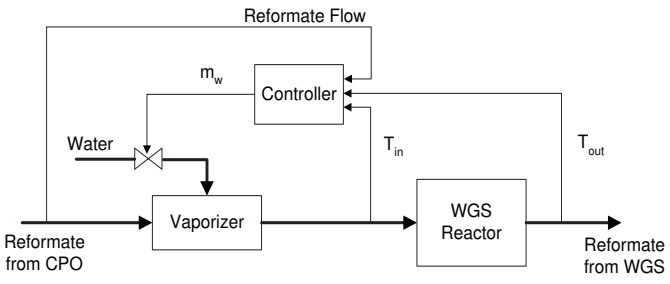

Fig. 2. Closed loop configuration for the water injector (vaporizer) and high temperature shift reactor subsystem

scheduling methods was compared experimentally on a lab scale WGS reactor with that of a nonlinear model predictive controller (NMPC) designed in [8]. The control of fuel and air flows into the FPS to regulate the CPO reactor temperature and H_2 delivery to the fuel cell stack has been studied in [9], [10]. The control of PROX reactors using neural networks has been studied in [11]. Control of air delivery to the cathode side of the fuel cell are studied in [12], [13].

In this paper, we employ the linear quadratic regulator (LQR) technique to design a multivariable controller for the vaporizer and WGS reactor subsystem that determines the the water injection rate from the available measurements. The closed loop setup for the system is shown in Figure 2. We introduce the system model and formulate the control problem in Section II. The LQR compensator design, including the state feedback controller and the state estimator steps, is discussed and the impact of various sensors on the observability of the system is discussed in Section III. Closed loop simulations on the nonlinear model showing the disturbance rejection performance are also presented. In Section IV, three different decentralized control architectures are evaluated based on the LQR compensator.

II. System model and control problem formulation

The plant, which in this case is a subsystem of the fuel processing system, is described by a nonlinear dynamic model. The water injection and water gas shift reactor subsystem is created in the Modelica modeling language (see [14]), using the component model library developed at UTRC for system level dynamic modeling of fuel cell power plants [15]. The reformate from the upstream CPOX is modeled as a constant composition stream coming from a source reservoir. The source flowrate varies based on the load requirement of the power plant. Downstream conditions are given by a fixed pressure sink model.

The water injector model has a liquid water phase with evaporation into the bulk gas phase to capture liquid holdup dynamics and two phase behavior. The separate liquid and gas volume models are multinode, i.e. described as a series of well-mixed volumes each with mass and energy balances. The mass and heat transfer between the two phases are described by relatively simple expressions, with parameters fitted to proprietary data.

The water-gas shift reactor model also uses a multinode discretization, corresponding to a series of CSTR (continuous-stirred tank reactors). The kinetics is described by a proprietary rate expression that approaches the shift reaction equilibrium. The model also incorporates heat transfer to the solid catalyst support.

In the vaporizer and WGS reactor subsystem, water injection rate is the actuated variable and the temperatures at the inlet and exit of the reactor are taken as measured outputs and the CO conversion is used as a performance output (unmeasured). This results in a non-square control problem. The measurement of the inlet reformate flow or an equivalent signal is assumed for disturbance feedforward control [16].

The full order nonlinear model is linearized around three different operating points corresponding to low (0%, idle), medium (50%) and high (100%) power levels of the powerplant to obtain linearized models of the form:

$$\dot{x} = Ax + Bm_w + B_d I_d \quad (1)$$

$$y = Cx \quad (2)$$

where x is the state vector, m_w is the input (water injection rate), I_d is the disturbance (reformate flowrate) and y is the output vector with CO conversion x_{CO}, WGS inlet and exit temperatures (T_{in} and T_{out}). The output x_{CO} enters the cost function but is not a measurement available for state estimation (see Section III). The order of the linear model is reduced to a tractable size using the balanced truncation approximation (BTA) model reduction algorithm from the SLICOT library [17]. A consequence of such model reduction is that the components of the state x no longer correspond to physical variables of the model. From here on, the matrices A, B, B_d and C refer to those of the reduced order model.

The step response and frequency response of the open loop reduced order plant to scaled input variables at three different power levels are shown in Figures 3 and 4 respectively. It can be seen that the plant behavior is quite different at low power due to nonlinearity.

The control objective is to ensure that thermal constraints are satisfied and adequate CO conversion is achieved. The inlet temperature signal contains thermal as well as stoichiometric information since the amount of cooling achieved is indicative of the amount of water added. The exit temperature represents the operating temperature and the equilibrium limit on conversion. The difference between the temperatures indicates the extent of reaction or CO conversion achieved. Since the reaction is reversible, exothermic and equilibrium limited, having more water in the feed and a lower operating temperature accelerates the WGS reaction. However, overcooling the gas stream reduces the catalyst activity and entrainment of liquid water damages the catalyst. On the other hand, high temperatures result in poor conversion (due to the equilibrium limitation) and may even damage the catalyst. Hence, the controller needs to maintain the balance

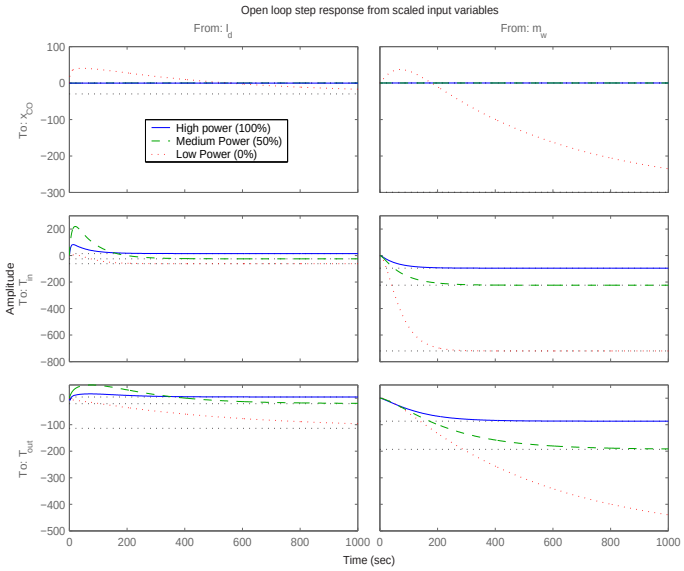

Fig. 3. Step response of the open loop plant at three power levels to scaled input variables

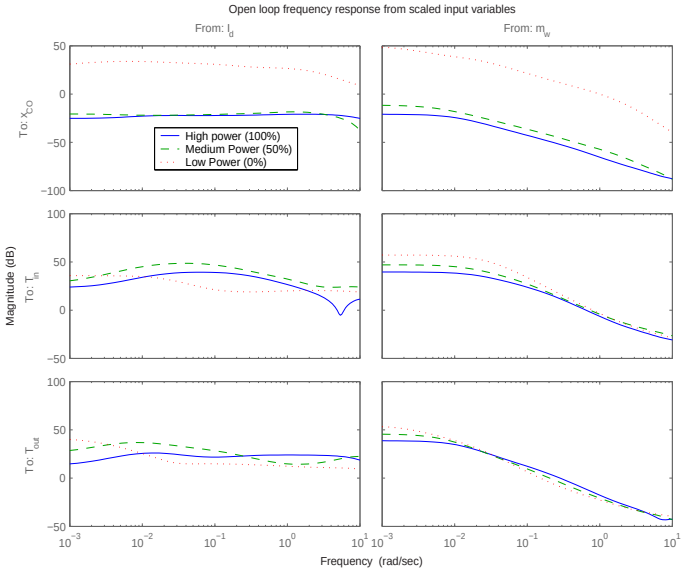

Fig. 4. Bode magnitude diagram of open loop plant at three power levels to scaled input variables

between achieving the desired CO conversion and satisfying the thermal constraints. In order to understand this tradeoff, we perform a multivariable controller design using the inlet and exit temperature measurements as well as the inlet reformate flow and study the effect of controller architecture on the closed loop disturbance rejection performance.

III. LQR COMPENSATOR DESIGN

We now describe the LQR compensator design based on the linear model and the control objectives described in Section II. The control design and closed loop simulations are performed using MATLAB™/Simulink™. The compensator consists of

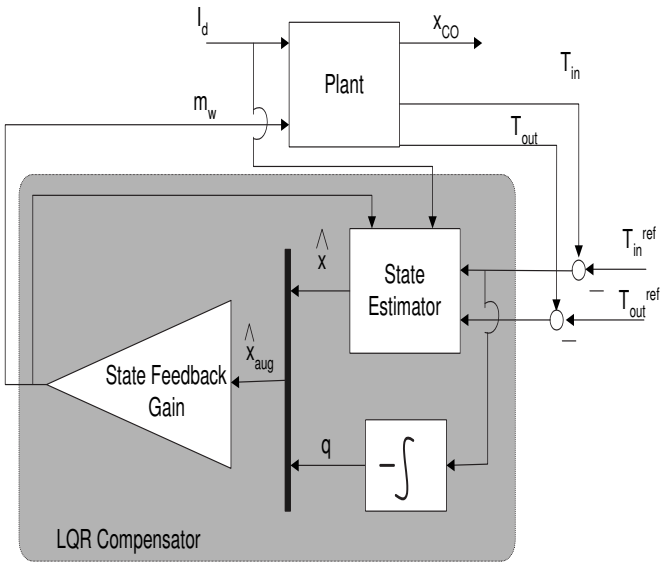

Fig. 5. Schematic of the LQR compensator showing the state feedback gain K_{aug} for the augmented system, the state estimator and the tracking state, q. T_{in}^{ref} and T_{out}^{ref} are the temperature reference signals.

a state feedback controller which is a constant gain matrix and a state estimator as shown in Figure 5. We consider T_{in} as the primary control variable since it responds faster to the disturbance. Other designs with T_{out} as the primary control variable are possible as the cascade architecture considered in [7].

In order to ensure zero offset in the primary controlled variable, T_{in}, the system model is augmented with a tracking state, q defined by

$$\dot{q} = T_{in}^{ref} - T_{in}.$$

The output vector is also augmented with q at the top. Note that the only exogenous signal relevant for LQR state feedback control design is the manipulated variable $u = m_w$. Hence, we drop the disturbance signal I_d and the reference signal T_{in}^{ref} from the dynamics for simplicity.

The augmented system dynamics is given by

$$\dot{x}_{aug} = A_{aug}x_{aug} + B_{aug}u$$

where

$$x_{aug} = \begin{bmatrix} x \\ q \end{bmatrix}, A_{aug} = \begin{bmatrix} A & 0 \\ -c_2 & 0 \end{bmatrix}, B_{aug} = \begin{bmatrix} B \\ 0 \end{bmatrix}$$

and c_i denotes the i-th row of C.

We define the output of the augmented system to include the signals to be penalized in the cost function:

$$y_{aug} = \begin{bmatrix} T_{in} \\ x_{CO} \\ q \end{bmatrix} = \begin{bmatrix} c_2 & 0 \\ c_1 & 0 \\ 0 & 1 \end{bmatrix} x_{aug}$$

The cost function to be minimized is defined as

$$J = \int_0^\infty (x'_{aug}Qx_{aug} + u'Ru)dt.$$

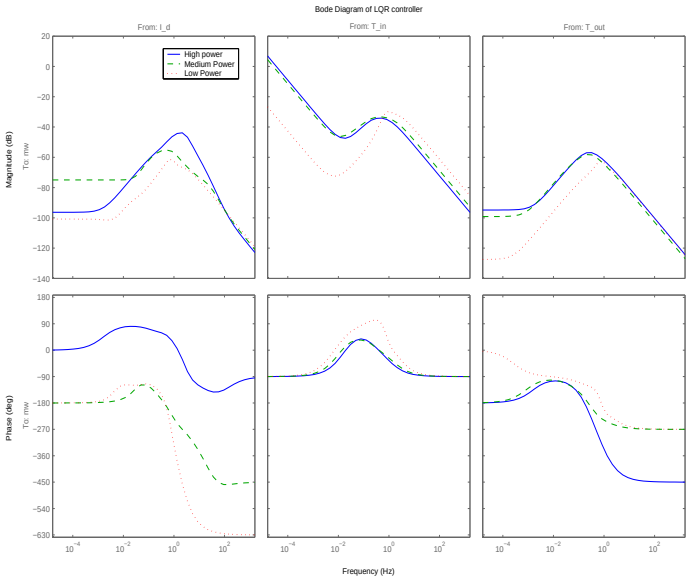

Fig. 6. Bode magnitude and phase diagrams of the 3×1 LQR compensator at three different power levels

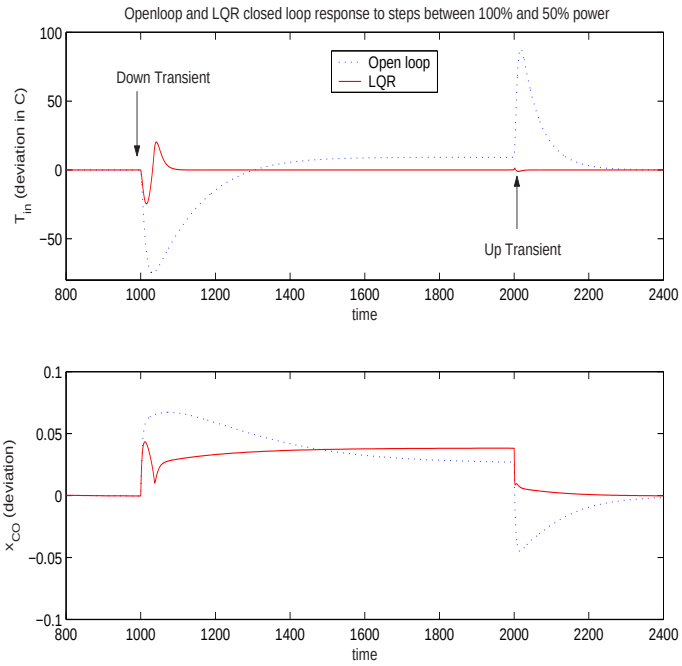

Fig. 7. Disturbance rejection performance of the LQR compensator in nonlinear simulation. The poor performance during down transient is due to actuator saturation. Temperature unit is K.

with $Q = \mathrm{diag}(c_1' Q_1 c_1, c_2' Q_2 c_2, Q_3)$. Here, Q_i $(i = 1, 2, 3)$ are scalar weights for x_{CO}, T_{in} and q respectively and R is the scalar weight on $u = m_w$. Note that penalizing only T_{in} and m_w does not capture the reactor performance as both signals are upstream of the reactor. The state feedback gain matrix, K_{aug}, is computed at three different power levels using the routine `lqr`.

An observer for estimating the states, x, of the reduced order model in Eqs 1–2 similarly designed using the routine `kalman`. The inputs to the estimator are the measured disturbance (I_d), the control input (m_w), the reactor inlet and exit temperatures (T_{in} and T_{out}). The state feedback gain K_{aug} is combined with the state estimator as shown in Figure 5 to obtain the overall compensator. The frequency response of the 3×1 compensator at three power levels is shown in Figure 6.

The performance of the linear compensator is verified by simulating on the nonlinear plant model. Since the water injection rate, m_w cannot be negative, actuator saturation needs to be accounted for with some anti-windup mechanism in the nonlinear implementation. A partial anti-windup scheme is implemented in the compensator by using the saturated m_w as input to the observer. The nonlinear closed loop response to a load disturbance from 100% power down to 50% power and then back to 100% power is shown in Figure 7.

A simple approach to quantify the impact of selected measurements on control and observability has been proposed in [10], [18]. Let $Q_{obs,C}$ denote the observability Gramian of the system with the measurements selected in the matrix C and let $\mathrm{cond(Q)}$ be the condition number of Q. The normalized condition number of $Q_{obs,C=C_z}$ with a given set of measurements in C_z is defined as

$$\eta_{C_z} = \frac{\mathrm{cond}(Q_{obs,C=C_z})}{\mathrm{cond}(Q_{obs,C=I})}. \qquad (3)$$

TABLE I

NORMALIZED CONDITION NUMBER IN EQ 3 AT VARIOUS POWER LEVELS WITH AND WITHOUT T_{out} MEASUREMENT

Measurements →	T_{in}	T_{in}, T_{out}
Low Power (0%)	1,055,306.8	121,060.8
Medium Power (50%)	64,500.4	125.6
High Power (100%)	230905.6	104.5

Note that $C = I$ implies that all states are measured. Thus, when η_{C_z} is small (*i.e.*, close to unity), the system is strongly observable and when $\eta_{C_z} \gg 1$, the system is weakly observable. Table I compares η_{C_z} for the vaporizer and WGS reactor subsystem with and without the outlet temperature measurement.

IV. CONTROLLER ARCHITECTURE EVALUATION

We now compare the performance of the three input, one output LQR controller with that of two decentralized controllers derived from the LQR controller. By dropping the third term of the LQR controller, we obtain a controller that uses the inlet temperature and the reformate inlet flow only. Such a controller, for example, can be realized as a PID controller on T_{in} with disturbance feedforward from I_d. By dropping two terms and retaining only the T_{in} term in the controller, we obtain a SISO feedback controller with no disturbance feedforward. The closed loop disturbance rejection performance of these three controllers is compared in Figure 8. It can be seen that the two term controller adequately recovers the performance of the LQR controller and the exit temperature measurement

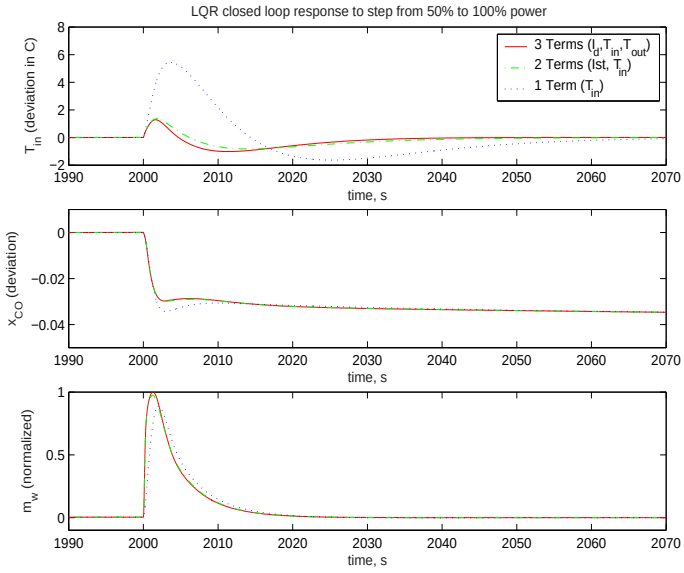

Fig. 8. Closed loop disturbance rejection performance with different control architectures derived from the LQR compensator. The temperature unit is K.

gives no significant improvement in performance.

V. Conclusion

Multivariable control design for the WGS reactor of a fuel processor is presented. The control problem is to manipulate the water injection rate so that good CO conversion is achieved and the thermal constraints are satisfied. An LQR compensator is designed at three different power levels with a cost function that includes CO conversion, inlet temperature deviation and the control effort. The linear compensator, with some anti-windup logic, is tested against the nonlinear model and the disturbance rejection performance is validated. Two decentralized controllers are derived from the multivariable controller and compared. This comparison reveals that regulation of inlet temperature with disturbance feedforward control is adequate. The reactor exit temperature measurement gives negligible improvement in control performance. It is shown that the system observability is improved by the exit temperature measurement.

References

[1] J. Larminie and A. Dicks, *Fuel Cell Systems Explained*, 2nd ed. John Wiley & Sons, 2003.

[2] L. Carrette, K. A. Friedrich, and U. Stimming, "Fuel cells– fundamentals and applications," *Fuel Cells*, vol. 1, no. 1, pp. 5–39, 2001.

[3] A. K. Avci, D. L. Trimm, and Z. I. Onsan, "Quantitative investigation of catalytic natural gas conversion for hydrogen fuel cell applications," *Chemical Engineering Journal*, vol. 90, pp. 77–87, 2002.

[4] J. M. Zalc and D. G. Loffler, "Fuel processing for PEM fuel cells: transport and kinetic issues of system design," *Journal of Power Sources*, vol. 111, pp. 58–64, 2002.

[5] P. S. Maiya, T. J. Anderson, R. L. Mieville, J. T. Dusek, J. J. Picciolo, and U. Balachandran, "Maximizing h_2 production by combined partial oxidation of ch4 and water gas shift reaction," *Applied Catalysis A: General*, vol. 196, pp. 65–72, 2000.

[6] K. Ukai *et al.*, "Hydrogen forming device," US Patent Application, US2003/0108456A1, 2003.

[7] C. Ling and T. F. Edgar, "Real-time control of a water-gas shift reactor by a model-based fuzzy gain scheduling technique," *J. Process Control*, vol. 7, no. 4, pp. 239–53, Aug 1997.

[8] G. T. Wright and T. F. Edgar, "Nonlinear model predictive control of a fixed-bed water-gas shift reactor: an experimental study," *Computers & Chemical Engineering*, vol. 18, no. 2, pp. 83–102, Feb 1994.

[9] J. T. Pukrushpan, A. Stefanopoulou, H. Peng, S. Varigonda, L. M. Pedersen, and S. Ghosh, "Control of natural gas catalytic partial oxidation for hydrogen generation in fuel cell applications," *IEEE Trans. Contr. Syst. Tech*, (to appear).

[10] S. Varigonda, J. T. Pukrushpan, and A. Stefanopoulou, "Challenges in fuel cell power plant control: The role of system level dynamic models," in *AIChE Spring Meeting*, New Orleans, 2003.

[11] L. C. Iwan and R. F. Stengel, "The application of neural networks to fuel processors for fuel-cell vehicles," *IEEE Transactions on Vehicular Technology*, vol. 50, no. 1, pp. 125–43, Jan 2001.

[12] J. T. Pukrushpan, A. Stefanopoulou, and H. Peng, "Modeling and control for PEM fuel cell stack system," in *Proc. of the ACC*, Anchorage, AK, 2002, pp. 3117–3122.

[13] S. Rodatz, G. Paganelli, and L. Guzzella, "Optimizing air supply control of a PEM fuel cell system," in *Proc. of the ACC*, vol. 3, Denver, 2003, pp. 2043–8.

[14] M. Tiller, *Introduction to Physical Modeling With Modelica*, ser. International Series in Engineering and Computer Science, 615. Kluwer, 2001. [Online]. Available: http://www.modelica.org

[15] J. Eborn, L. Pedersen, C. Haugstetter, and S. Ghosh, "System level dynamic modeling of fuel cell power plants," *Proceedings of the 2003 American Control Conference*, pp. 2024–2029, 2003.

[16] G. Stephanopoulos, *Chemical Process Control: An Introduction to Theory and Practice*. Prentice-Hall, 1990.

[17] P. Benner, V. Mehrmann, V. Sima, S. Van Huffel, and A. Varga, *SLICOT– A Subroutine Library in Systems and Control Theory*. Birkauser, 1999, vol. 1, ch. 10, pp. 499–539. [Online]. Available: http://www.win.tue.nl/niconet/NIC2/slicot.html

[18] J. T. Pukrushpan, "Modeling and control of fuel cell systems and fuel processors," Ph.D. dissertation, University of Michigan, Ann Arbor, 2003.